Supramolecular Chemistry
Publication details, including instructions for authors and subscription information:
http://www.informaworld.com/smpp/title~content=t713649759

N-H...O Assisted Structural Changes Induced on Ketoenamine Systems

M. Rodríguez[a]; R. Santillan[a]; Y. López[a]; N. Farfán[b]; V. Barba[c]; K. Nakatani[d]; E. V. García Baéz[e]; I. I. Padilla-Martínez[e]

[a] Departamento de Química, Centro de Investigación y de Estudios Avanzados del IPN, México [b] Facultad de Quimica, Departamento de Quimica Orgánica, Universidad Nacional Autónoma de México, México D. F., 04510, México [c] Centro de Investigaciones Químicas, Universidad Autónoma del Estado de Morelos, México [d] Laboratoire de Photophysique et Photochimie Supramoléculaire et Macromoléculaire, Ecole Normale Supérieure de Cachan, France [e] Departamento de Química, Unidad Profesional Interdisciplinaria de Biotecnología, Instituto Politécnico Nacional, México

To cite this Article Rodríguez, M. , Santillan, R. , López, Y. , Farfán, N. , Barba, V. , Nakatani, K. , Baéz, E. V. García and Padilla-Martínez, I. I.(2007) 'N-H...O Assisted Structural Changes Induced on Ketoenamine Systems', Supramolecular Chemistry, 19: 8, 641 — 653
To link to this Article: DOI: 10.1080/10610270701534778
URL: http://dx.doi.org/10.1080/10610270701534778

Supramolecular Chemistry, December 2007 Vol. 19 (8), pp. 641–653

Taylor & Francis
Taylor & Francis Group

N—H···O Assisted Structural Changes Induced on Ketoenamine Systems

M. RODRÍGUEZ[a], R. SANTILLAN[a,*], Y. LÓPEZ[a], N. FARFÁN[b], V. BARBA[c], K. NAKATANI[d], E. V. GARCÍA BAÉZ[e] and I. I. PADILLA-MARTÍNEZ[e]

[a]*Departamento de Química, Centro de Investigación y de Estudios Avanzados del IPN, México;* [b]*Facultad de Quimica, Departamento de Quimica Orgánica, Universidad Nacional Autónoma de México, México D. F., 04510, México;* [c]*Centro de Investigaciones Químicas, Universidad Autónoma del Estado de Morelos, México;* [d]*Laboratoire de Photophysique et Photochimie Supramoléculaire et Macromoléculaire, Ecole Normale Supérieure de Cachan, France;* [e]*Departamento de Química, Unidad Profesional Interdisciplinaria de Biotecnología, Instituto Politécnico Nacional, México*

(Received 1 March 2007; Accepted 25 June 2007)

The tautomeric equilibrium between the ketoenamine and enolimine forms for a series of arylimines (1a–1c) derived from salicylaldehyde and enaminones (2a–2f) derived from benzoylacetone and substituted anilines has been analyzed in solution by ^{1}H NMR and UV-vis spectroscopy, while IR and X-ray diffraction analyses were used in the solid state. The X-ray diffraction analysis of 1a, 2a–2c and 2e–2f showed that the most stable tautomer is the ketoenamine and all enaminones present intramolecular NH···O hydrogen bonds forming a six member ring in which the keto form is favored. In addition, the VT-NMR analysis for 2b in solvents of different polarities evidenced the behavior of the tautomeric equilibrium, showing that in DMF and acetone at low temperature, the enolimine tautomer is more stable.

Keywords: Enaminones; Imines; X-ray; VT-NMR; RAHB

INTRODUCTION

Schiff bases are important in several fields of chemistry and biochemistry owing to their biological activity [1,2] and can be classified according to their photochromic or thermochromic properties [3,4]. Some arylimine derivatives of salicylaldehyde have attracted the interest of chemists and physicists due to their reversible photo- or thermoreactivity in the solid state. For instance, the thermochromic properties of N-salicylidenanilines have been attributed to *enolimine-ketoenamine* tautomerism. The first evidence of a keto-enol equilibrium in the solid state was given by Ogawa *et al.* [5] who reported the variable temperature X-ray analysis of N-(5-chloro-2-hydroxybenzylidene)-4-hydroxyaniline (**A**) (Fig. 1) detecting the presence of both tautomers (10% for the Enol and 90% of the Keto tautomer).

Furthermore, Ogawa *et al.* [6] reported the thermochromic properties of salicylidenaniline in nonpolar solvent solutions showing that proton movement between the nitrogen and oxygen atoms is responsible for the electronic transfer which is also controlled by the aggregation state of the molecules.

The photonic properties of arylimines derived from salicylaldehyde (Fig. 2) have been related to proton transfer reactions in the solid state and investigated for **B** and **C**, which present a color change upon irradiation under UV light. The yellow color is attributed to the *enol* form, the most stable species, while the red color corresponds to the excited state and appears after irradiation. As a result, these derivatives have been used as molecular switches to modulate their optoelectronic properties, specifically the second harmonic generation in the solid state for molecules that crystallize in non centrosymmetric space groups [7].

Compounds containing the N(sp^3)—C(sp^2)=C(sp^2)—C(sp^2)=O(sp^2) fragment which is bonded by strong hydrogen bonds (N—H···O or N···H—O), are known as enaminones. These compounds are characterized by the presence of NH or OH moieties, which are of biological interest [8,9] because they play an important role in molecular recognition. They are also synthetic intermediates in organic

*Corresponding author. E-mail: rsantill@cinvestav.mx.

ISSN 1061-0278 print/ISSN 1029-0478 online © 2007 Taylor & Francis
DOI: 10.1080/10610270701534778

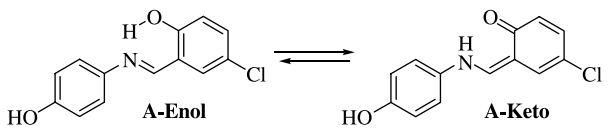

FIGURE 1 Tautomeric equilibrium in the solid state.

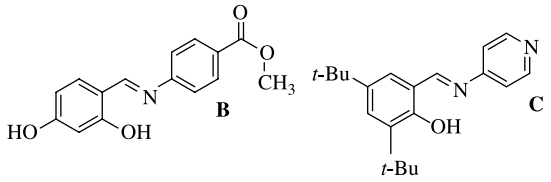

FIGURE 2 Arylimines with photochromic properties.

reactions [10,11] and have been used as sensor materials [12,13] with optoelectronic properties [14].

The strong hydrogen bond present in enaminones leads to the observation of tautomeric equilibria between the *enolimine* $\cdots N(sp^2)=C(sp^2)-C(sp^2)=C(sp^2)-O(sp^2)-H$ and *ketoenamine* $H-N(sp^2)-C(sp^2)=C(sp^2)-C(sp^2)=O(sp^2)\cdots$ species. These systems can be analyzed in terms of the well-known RAHB phenomenon (Resonance Assisted by Hydrogen Bond), an analysis over structural effects, mainly variation in bond distances, based on hydrogen position and delocalization of the π-electrons present in a fragment containing a donor and an acceptor group (nitrogen or oxygen atoms), such as that found in enaminones. The phenomenon was first observed by Gilli [15] in 1,3-diketones and applied to hetero-compounds containing nitrogen, such as imines or enaminones [16–18], as well as sulfur derivatives [19,20]. The relationship between the resonance effect and hydrogen bond has been analyzed in detail recently [21].

Other species where proton transfer reactions have been investigated by ^{1}H NMR in solution are 2-hydroxychalcones **D** (Fig. 3). These derivatives show a variation in the chemical shift of the HO signal at different temperatures, but no differences with changes in solvent polarity [22].

In continuation of our studies on Schiff base ligands, herein we describe an X-ray diffraction and spectroscopic study of the ketoenol tautomeric forms of six enaminones prepared from salicylaldehyde and substituted anilines.

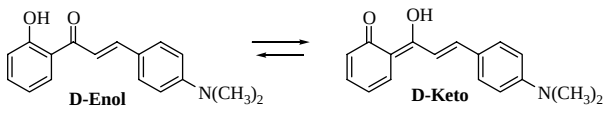

FIGURE 3 Proton transference reaction present in 2-hydroxychalcones.

EXPERIMENTAL PART

Instrumental

NMR studies were carried out with a Bruker Avance 300 instrument using TMS as standard (internal ^{1}H, ^{13}C). Chemical shifts are stated in parts per million; they are positive, when the signal is shifted to higher frequencies than the standard. COSY and HETCOR experiments have been carried out in order to assign the ^{1}H and ^{13}C spectra completely. IR spectra were recorded on a FT-IR Perkin Elmer GX spectrophotometer. Mass spectra were obtained on HP 5989A equipment and UV spectrum were obtained on a Varian Carry UV-Vis 4000 spectrometer. Elemental analyses were carried out on a Finnigan Flash EA 1112. The single crystal X-ray diffraction analyses were realized on a Kappa CCD diffractometer. Solution and refinement: direct method SHELX-92 for structure solution and the SHELXL-97 software package for refinement and output data [23].

Commercially available salicylaldehyde, benzoylacetone, anilines (*2*-amino-*6*-methylphenol, *o*-aminophenol, *3*-aminophenol, *4*-aminophenol, *4*-ethanolaniline *4*-aminobenzoic acid) and the solvents were used without further purification. Compounds **1a**, **1b** and **1c** were prepared as described in the literature [24].

General Procedure for the Preparation of Enaminones 2a–2f

Equimolar quantities of the corresponding aniline and benzoylacetone were heated under reflux in methanol (25 ml) for 120 min. Part of the solvent and water formed during the reaction were removed with a Dean-Stark trap to yield a colored solid which was recrystallized several times in methanol solution.

3-(2-Hydroxy-4-methylphenylamino)-1-phenyl-but-2-en-1-one (2a)

The title compound was prepared from 1.60 g (10.0 mMol) of benzoylacetone and 1.20 g (10 mMol) of 2-amino-5-methylphenol to give 2.30 g (8.60 mMol, 87% yield) of **2a** as a yellow solid. M.p.: 189–190°C.

IR$\bar{\nu}_{max}$ (KBr): 3784, 3154, 2962, 1602, 1574, 1427, 1327, 1219, 1118, 1027, 759 cm^{-1}. ^{1}H NMR (300 MHz, $CDCl_3$) δ: 1.66 (3H, s, H-1), 2.31 (3H, s, 12-Me), 5.70 (1H, s, H-3), 6.67 (1H, d, J = 7.0 Hz, H-14), 6.70 (1H, s, H-11), 6.90 (1H, d, J = 7.0 Hz, H-13), 7.41 (3H, m, H-7,8), 7.88 (2H, d, J = 7.0 Hz, H-6), 12.32 (1H, s, NH) ppm. ^{13}C NMR (75 MHz, $CDCl_3$) δ: 20.1 (C-1), 21.5 (C-Me), 94.7 (C-3), 118.0 (C-14), 121.0 (C-11), 122.8 (13), 127.6 (C-6, 12), 128.6 (C-7), 131.2 (C-8), 139.3 (C-9), 140.3 (C-5), 152.3 (C-10), 165.9 (C-2), 188.7

(C-4) ppm. MS (20 eV) m/z (%): 267 (M^+, 20), 266 (15), 252 (7), 210 (4), 190 (5), 148 (100), 105 (50), 77 (37). Anal. Calc. for $C_{17}H_{17}NO_2$: C, 75.87; H, 6.97; N, 5.53. Found: C, 75.22; H, 6.10; N, 5.22.

3-(2-hydroxy-phenylamino)-1-phenylbut-2-en-1-one (2b)

The title compound was prepared from 1.00 g (6.16 mMol) of benzoylacetone and 0.67 g (6.16 mMol) of *o*-aminophenol to give 1.34 g (5.29 mMol, 85% yield) of **2b** as a yellow solid. M.p.: 165–168°C.

IR$\bar{\nu}_{max}$ (KBr): 3238, 1573, 1539, 1455, 1327, 1282, 1096, 752 cm^{-1}. ^1H NMR (300 MHz, $CDCl_3$), δ: 1.60 (3H. s, H-1), 5.65 (1H, s, H-3), 6.85 (1H, td, J = 8.5, 1.0 Hz, H-12), 7.03 (1H, dd, J = 8.5, 1.0 Hz, H-14), 7.05 (1H, dd, J = 8.5, 1.0 Hz, H-11), 7.19 (1H, td, J = 8.5, 1.0 Hz, H-13), 7.41–7.47 (3H, m, H-7, H-8), 7.89 (2H, d, J = 7.6 Hz, H-6), 8.90 (1H, s, H—OH), 12.40 (1H, s, H—NH) ppm; ^{13}C NMR (75 MHz, $CDCl_3$) δ: 20.1 (C-1), 94.9 (C-3), 117.7 (C-14), 120.2 (C-11), 125.4 (C-9), 127.7 (C-6), 127.9 (C-12), 128.7 (C-7), 129.0 (C-13), 131.3 (C-8), 140.2 (C-5), 152.8 (C-10), 165.9 (C-2), 188.7 (C-4) ppm; MS (20 eV) m/z (%): 253 (M^+, 24), 252 (29), 238 (11), 134 (100), 105 (57) 77 (14). Anal. Calc. for $C_{16}H_{15}NO_2$: C, 75.87; H, 5.97; N, 5.53. Found: C, 75.88; H, 6.37; N, 5.64.

(Z)-3-(3-Hydroxyphenylamino)-1-phenylbut-2-en-1-one (2c)

The title compound was prepared from 1.62 g (10 mMol) of benzoylacetone and 1.09 g (10 mMol) of 3-aminophenol to give 2.21 g (8.7 mMol, 87% yield) of **2c** as a yellow solid. M.p.: 136–138°C.

IR$\bar{\nu}_{max}$ (KBr): 3360, 3295, 3028, 2954, 1574, 1539, 1464, 1302, 1258, 1176, 1149, 906, 770, 688 cm^{-1}. ^1H NMR (300 MHz, $CDCl_3$) δ: 1.99 (3H, s, H-1), 5.70 (1H, s, H-3), 6.45–6.56 (3H, m, H-10, 12, 14), 6.70 (1H, dd, J = 7.8, 7.9 Hz, H-13), 7.22–7.34 (3H, m, H-7, 8), 7.72 (2H, d, J = 7.8 Hz, H-6) ppm. ^{13}C NMR (75 MHz, $CDCl_3$) δ: 20.0 (C-1), 93.6 (C-3), 111.3 (C-10), 112.7 (C-12), 115.0 (C-14), 126.5 (C-6), 127.8 (C-7), 129.4 (C-13), 130.4 (C-8), 138.9 (C-9), 139.4 (C-5), 157.6 (C-11), 162.1 (C-2), 187.6 (C-4) ppm. MS (20 eV) m/z (%): 253 (M^+, 60), 252 (80), 148 (100), 133 (20), 105 (80), 77 (30) Anal. Calc. for $C_{16}H_{15}NO_2$: C, 75.87; H, 5.97; N, 5.53. Found: C, 75.75; H, 6.11; N, 5.50.

(Z)-1-Phenyl-3-(4-hydroxyphenylamino)-1-phenyl but-2-en-1-one (2d)

The title compound was prepared from 1.62 g (10 mMol) of benzoylacetone and 1.09 g (10 mMol) of 4-aminophenol to give 2.30 g (8.0 mMol, 92% yield) of **2d** as a yellow solid. M.p.: 192–194°C.

IR$\bar{\nu}_{max}$ (KBr): 3320, 3102, 2927, 1616, 1578, 1510, 1443, 1328, 1221, 1240, 760, 717 cm^{-1}. ^1H NMR (300 MHz, DMSO-d_6) δ: 2.10 (3H, s, H-1), 6.00 (1H, s, H-3), 6.79 (2H, d, J = 8.6 Hz, H-11), 7.11 (2H, d, J = 8.6 Hz, H-10), 7.42–7.52 (3H, m, H-7, 8), 7.90 (2H, d, J = 8.4 Hz, H-6), 9.60 (NH) ppm. ^{13}C NMR (75 MHz, DMSO-d_6) δ: 25.3 (C-1), 98.3 (C-3), 121.3 (C-11), 131.7 (C-10), 132.3 (C-6), 133.9 (C-7), 134.4 (C-9), 136.4 (C-8), 145.1 (C-5), 161.2 (C-12), 169.0 (C-2), 192.0 (C-4) ppm. MS (20 eV) m/z (%): 252 (M^+, 100), 238 (10), 176 (26). Anal. Calc. for $C_{16}H_{15}NO_2$: C, 75.87; H, 5.97; N, 5.53. Found: C, 75.79; H, 6.61; N, 5.52.

(Z)-1-Phenyl-3-(4-(2-hydroxyethane)phenylamino)-1-phenylbut-2-en-1-one (2e)

The title compound was prepared from 1.62 g (10 mMol) of benzoylacetone and 1.37 g (10 mMol) of 4-ethanolaniline to give 2.30 g (8.1 mMol, 81% yield) of **2e** as a yellow solid. M.p.: 120–122°C.

IR$\bar{\nu}_{max}$ (KBr): 3436, 2932, 1598, 1560, 1543, 1506, 1324, 1285, 1190, 1048, 835, 751, 719 cm^{-1}. ^1H NMR (300 MHz, $CDCl_3$) δ: 2.15 (3H, s, H-1), 2.88 (2H, t, J = 6.5 Hz, CH_2), 3.87 (2H, t, J = 6.5 Hz, CH_2—OH), 5.90 (1H, s, H-3), 7.12 (2H, d, J = 8.2 Hz, H-11), 7.24 (2H, d, J = 8.2 Hz, H-10), 7.41–7.50 (3H, m, H-7, 8), 7.93 (2H, dd, J = 2.1, 7.4 Hz, H-6), 13.00 (1H, s, NH) ppm. ^{13}C NMR (75 MHz, $CDCl_3$) δ: 20.8 (C-1), 39.0 (CH_2), 63.8 (CH_2O), 94.5 (C-3), 125.2 (C-10), 124.4 (C-6), 128.7 (C-7), 130.1 (C-11), 131.3 (C-8), 136.7 (C-12), 137.3 (C-9), 140.1 (C-5), 162.8 (C-2), 189.0 (C-4) ppm. MS (20 eV) m/z (%): 281 (M^+, 84), 280 (96), 250 (96), 158 (41), 105 (100), 77 (19). Anal. Calc. for $C_{18}H_{19}NO_2$: C, 76.84; H, 4.44; N, 4.71. Found: C, 76.67; H, 4.25; N, 4.96.

(Z)-1-Phenyl-3-(4-carboxyphenylamino)-1-phenyl but-2-en-1-one (2f)

The title compound was prepared from 1.62 g (10 mMol) of benzoylacetone and 1.37 g (10 mMol) of 4-aminobenzoic acid to give 1.90 g (6.70 mMol, 70% yield) of **2f** as a yellow solid. M.p.: 216–217°C.

IR$\bar{\nu}_{max}$ (cm^{-1}): 3467, 2819, 1679, 1590, 1567, 1422, 1319, 1280, 1181, 1064, 854, 794, 708 cm^{-1}. ^1H NMR (300 MHz, DMSO-d_6) δ: 2.30 (3H, s, H-1), 6.18 (1H, s, H-3), 7.40 (2H, d, J = 8.5 Hz, H-11) 7.47–7.55 (5H, m, H-10, 7, 8), 7.95 (2H, d, J = 8.1 Hz, H-6), 12.90 (1H, s, COO—H), 13.30 (1H,s, NH) ppm. ^{13}C NMR (75 MHz, DMSO- d_6) δ: 21.3 (C-1), 96.3 (C-3), 123.4 (C-10), 127.5 (C-12), 127.8 (C-6), 129.3 (C-7), 131.5 (C-11), 132.3 (C-8), 139.8 (C-5), 143.3 (C-9), 162.1 (C-2), 167.6 (COOH), 188.5 (C-4) ppm. MS (20 eV) m/z (%): 281 (M^+, 50), 280 (100), 204 (8), 176 (12), 160 (8), 132 (10), 105 (25), 77 (8). Anal. Calc. for; $C_{17}H_{15}NO_3$; C, 72.76, N, 4.92, H, 6.67 found; C, 72.58; N, 4.98; H, 5.37.

RESULTS AND DISCUSSION

Compounds **1a–1c** (Fig. 4) were prepared as described in the literature [24]. Arylimine **1a** was obtained as a red crystalline solid which differs in solubility and color from the related compounds **1b** and **1c** (both yellow solids); compound **1a** is soluble in polar solvents while **1b** and **1c** dissolve in solvents of low polarity. The crystals from **1a** were obtained from methanol and the spectroscopic data is in agreement with previous reports [24]. Arylenaminones **2a–2f** were prepared by reaction of benzoylacetone with the corresponding anilines and all products were solid. The IR analysis for **1a** showed a broad absorption band in 1680 cm^{-1} for the C═O bond which is indicative of hydrogen bonding; the N—H absorption presents a value close to 3560 cm^{-1} corresponding to a strong N—H···O interaction. Mass spectral analysis was obtained at 20 eV observing the molecular ion.

Derivatives **2a–2f** were characterized by ^{1}H NMR showing two singlets assigned to H-3 and the NH which are indicative of the formation of enaminones. The signal for the enamine proton (H-3) is in the range from 5.65 ppm to 6.20 ppm, while that of the NH proton appears in the range from 12.32 ppm to 13.30 ppm (Table I), characteristic of a strong hydrogen bond (N—H···O) [24]. The ^{13}C NMR spectra for **2a–2f** showed three characteristic signals, the enamine moiety in the range from 162.1 ppm to 169.0 ppm (C-2), C-4 between 187.7 ppm and 192.0 ppm, where the largest shifts correspond to compound **2d** and the signal for C-3 in the range from 93.6 ppm to 98.3 ppm. Unambiguous ^{13}C and ^{1}H assignment for all compounds was attained using two dimensional experiments (COSY, HETCOR and HMQC). For unequivocal assignment of the NH signal in the ^{1}H NMR spectra, the HMQC ^{1}H vs ^{15}N spectra for **2b** was obtained observing a correlation between nitrogen (−258 ppm) and the NH proton (12.40 ppm) signals (Fig. 5).

Based on the chemical shifts measured by ^{1}H and ^{13}C NMR, the most stable tautomer for derivatives **2a–2f** in solution is the ketoenamine form, nonetheless the ^{1}H NMR spectrum of **2b** in chloroform at low concentration showed signals assigned to the enolimine tautomer (**2b-enol**). In order to investigate the tautomeric equilibrium (Fig. 6) present in **2b** [25], VT-NMR measurements in different solvents were carried out. The variation in N—H chemical shift with respect to temperature is shown in Fig. 7. The results show that at 300 K the N—H chemical shift is close to 12.40 ppm in solvents with low dielectric constant and shifts near 13.00 ppm in high dielectric constant solvents, indicating a stronger N—H···O hydrogen bond formation in these last solvents. The NH signal is shifted to lower frequencies in chloroform and methylene chloride and to higher frequencies in acetone and dimethylformamide at low temperature.

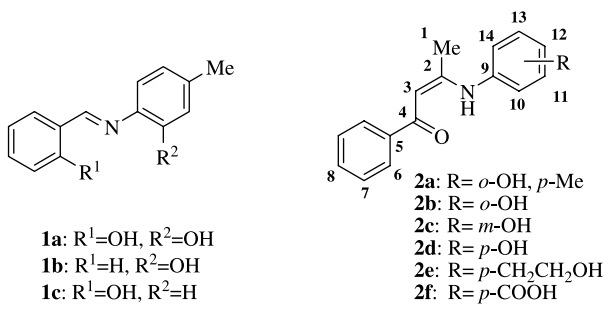

FIGURE 4 Arylimines (**1a–1c**) and arylenaminones (**2a–2f**) derived from salicylaldehyde or benzoylacetone and anilines.

TABLE I ^{1}H and ^{13}C chemical shift for **2a–2f**

	^{1}H NMR (ppm)			^{13}C NMR (ppm)		
	H-1	H-3	NH	C-2	C-3	C-4
2a	1.66	5.70	12.32	165.9	94.7	188.7
2b-keto	1.60	5.65	12.40	165.9	94.9	188.7
2b-enol	2.22	6.20	16.28	165.9	94.9	188.7
2c	1.99	5.70	12.38	162.1	93.6	187.6
2d	2.10	6.00	9.60	169.0	98.3	192.0
2e	2.15	5.90	13.00	162.8	94.5	189.0
2f	2.30	6.18	13.30	162.1	96.3	188.5

Figure 8 shows the influence of temperature on the chemical shift for H-1 (CH_3 protons); in polar and non polar solvents and at low temperatures. The shift of NH, H-1 and H-3 to higher frequency in acetone and dimethylformamide at low temperature is indicative of π electronic delocalization in the N—C—C—C—O fragment. Generally, the N—H···O hydrogen bond of enaminones leads to six-membered heterocyclic ring formation. In addition, if a π system is present, it is capable of exhibiting Resonance Assisted by Hydrogen Bonding, which can be defined as a positive synergism between hydrogen bond strengthening and π-delocalization of the interleaving resonance fragment.

The influence of a second hydrogen transfer on the stabilization of the ketoenamine tautomer in Schiff bases **1a**, **1b**, **1c** and **2a** was evaluated by UV-vis spectroscopy in toluene. Absorption bands corresponding to intramolecular N—H···O and a second intermolecular O—H···O hydrogen bond were observed at 360 nm and 341 nm for **1a** and **2a**, respectively; this band is reduced significantly for compound **1b** and **1c**, where R^1═H, R^2═OH and R^1═OH, R^2═H, respectively (Fig. 9).

X-ray Analysis of Compounds 1a, 2a–c, 2e and 2f

Compound **1a** crystallizes in the space group $P2_1/c$ as a monoclinic system with four molecules in the unit cell. Compounds **2a**, **2c** and **2e** crystallize in the space group P-1 as triclinic system with two

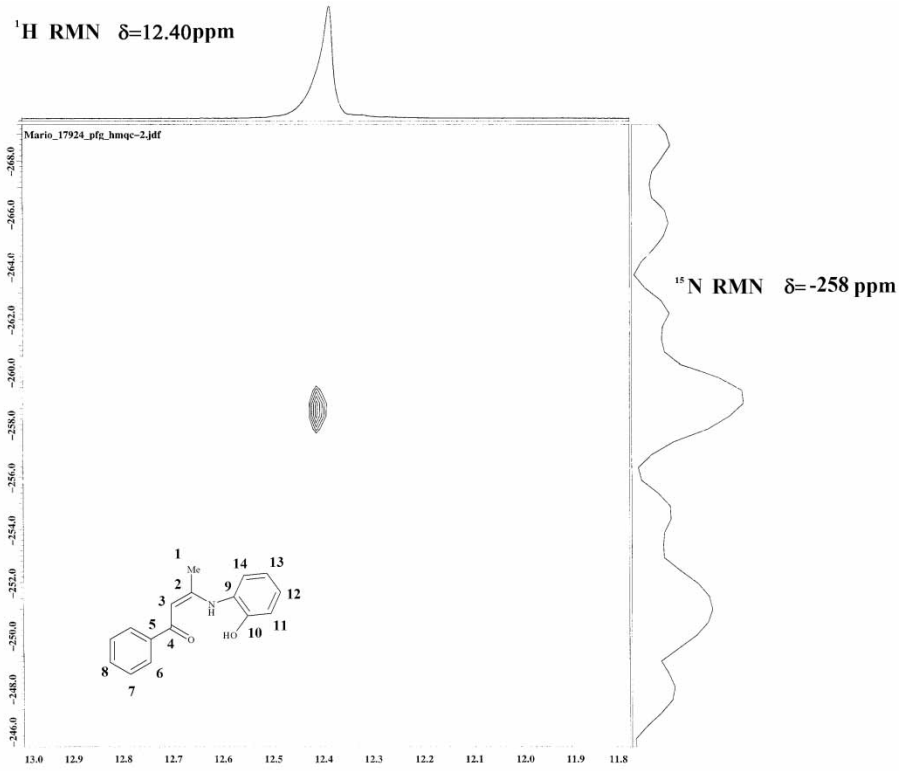

FIGURE 5 HMQC spectrum (^{15}N vs ^{1}H) of **2b**. Correlation of the proton signal (12.40 ppm) with the nitrogen signal (−258 ppm), the experiment was obtained employing J = 80 Hz.

molecules in the unit cell while **2b** contains four molecules in the unit cell and two independent molecules in the asymmetric unit. Compound **2f** was crystallized as two polymorphs, both crystallized in the space group $P2_1/c$ with four molecules in the unit cell but with different dimensions: a = 8.0610(2), b = 9.2814(2), c = 19.5993(2)Å, α = 90°, β = 110.303(10)° and γ = 90° for the polymorph denoted as **2f** and a = 11.8875(5), b = 11.1448(6), c = 12.1972(6) Å, α = 90°, β = 118.875(2)°, γ = 90° for the polymorph denoted as **2f′**. Crystal data collection and refinement for all compounds are listed in Table II.

X-ray Study of the Keto-imine Equilibrium in 1a

The molecular structure of compound **1a** is shown in Fig. 10, the bond distances are summarized in Table III. The X-ray structure of **1a** shows that at room temperature the ketoenamine form is more stable than the enolimine form, as evidenced by the changes in bond distances for the N(1)-C(7)-C(6)-C(1)-O(1) fragment. This keto-imine equilibrium has been previously studied by Ogawa *et al.* [5] in the solid state. These authors found a 90:10 ratio of keto-imine forms of *N*-(5-chloro-2-hydroxybenzylidene)-4-hydroxyaniline at 90 K and 69:31 ratio at 299 K, using X-ray diffraction experiments.

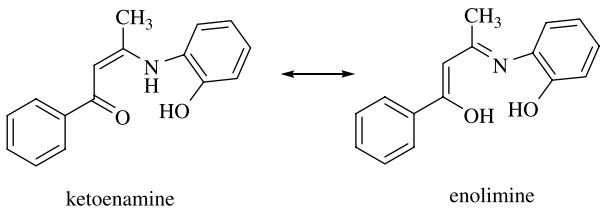

FIGURE 6 Tautomeric equilibrium present in enaminones.

The N═C and C(1)—O(1) bond distances have been taken as reference to establish the presence of a particular tautomer. A large N═C distance and a short C(1)—O(1) bond are related to the keto form; the opposite behavior is characteristic of the imine form. The C═N distance in **1a**, 1.323(6) Å, is larger than that of **B**, 1.2888(18) Å and **C**, 1.282(4) Å but similar to the one reported for the **A**-keto form (1.308(1) Å) [6]. As a result of proton transfer from oxygen to nitrogen, a variation in distance is expected, thus relative to the average $C(sp^2)$—$C(sp^2)$ bond distance of 1.49 Å and that of $C(sp^2)$═$C(sp^2)$ of 1.33 Å [26], the C(7)—C(6) bond in **1a** (1.395(7) Å) has an intermediate value between a single and a double C—C bond and is shorter than that observed for **A-keto**, **B** and **C** 1.425(2) Å, 1.440(2) Å and 1.448(5) Å, respectively. Another relevant distance indicative of the presence of the ketoenamine tautomer is the C(1)—O(1) bond, which showed the smallest value for **1a**, 1.297(6) Å compared to the distances observed

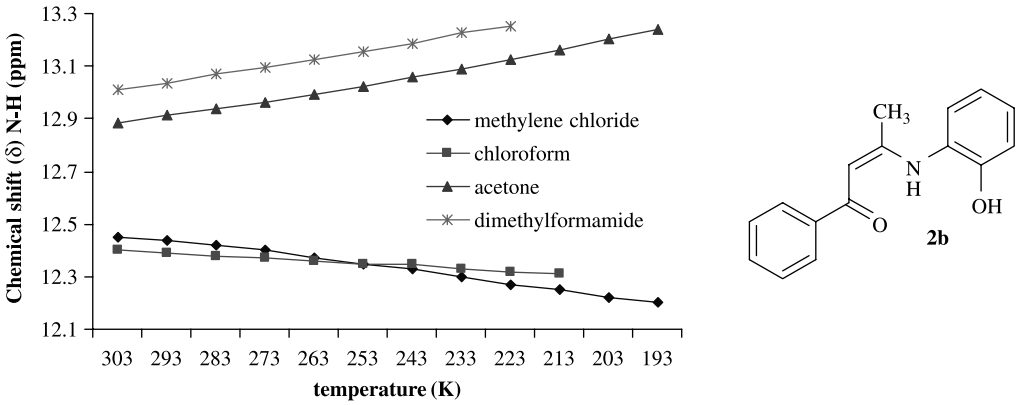

FIGURE 7 Variable temperature ^{1}H NMR data for the NH proton in **2b** using different solvents.

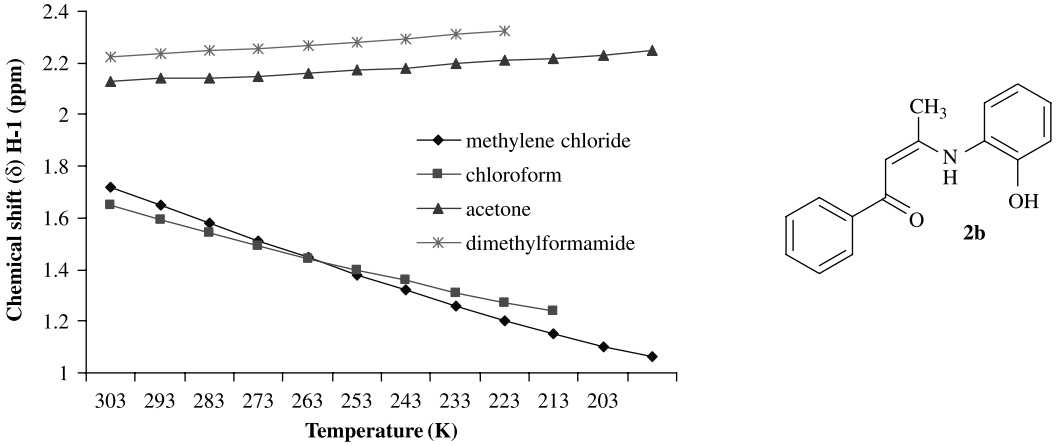

FIGURE 8 ^{1}H NMR data for H-1 (CH_3) in compound **2b** at different temperatures.

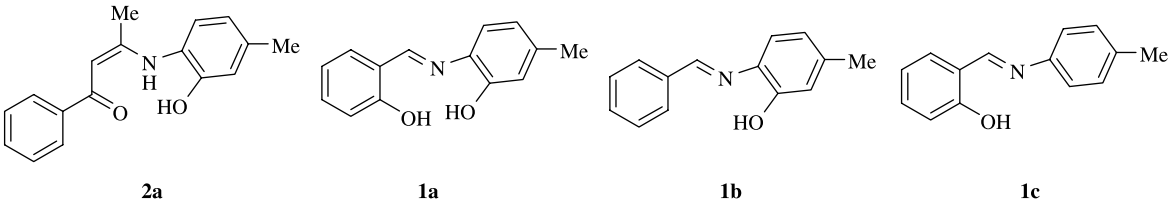

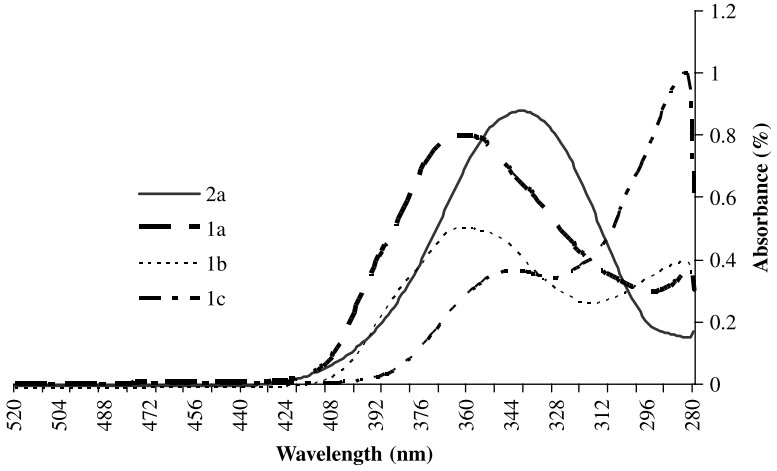

FIGURE 9 UV spectra for derivates **1a**, **1b**, **1c** and **2a** in toluene.

TABLE II Crystallographic data for compounds **1a**, **2a**, **2b** **2c**, **2e**, **2f** and **2f′**

Compound	**1a**	**2a**	**2b**	**2c**	**2e**	**2f**	**2f′**
Formula	$C_{10}H_{13}NO_2$	$C_{17}H_{17}NO_2$	$C_{16}H_{15}NO_2$	$C_{16}H_{15}NO_2$	$C_{36}H_{38}N_2O_4$	$C_{17}H_{15}NO_3$	$C_{17}H_{15}NO_3$
Size	0.48 0.40 0.24	0.37 0.25 0.2	0.31 0.24 0.19	0.29 0.25 0.22	0.32 0.28 0.21	0.45 0.30 0.25	0.75 0.45 0.37
F.W. (g/mol)	179.21	267.32	253.30	253.30	562.71	281.31	281.31
Space Group	$P2_1/c$	P-1	P-1	P-1	P-1	P21/c	P21/c
Crystal System	Monoclinic	Triclinic	Triclinic	Triclinic	Triclinic	Monoclinic	Monoclinic
a (Å)	10.072(2)	9.0614(3)	9.1920(2)	7.768(2)	8.6777(3)	8.0610(2)	11.8875(5)
b (Å)	8.267(2)	9.1109(2)	10.7401(2)	9.558(2)	9.6321(3)	9.2814(2)	11.1448(6)
c (Å)	11.780(2)	9.6974(3)	15.2514(4)	10.0948(10)	9.6566(3)	19.5993(5)	12.2494(5)
α (°)	90	62.213(2)	73.096(10)	99.526(15)	76.964(2)	90	90
β (°)	111.75(3)	85.2320(10)	79.231(10)	109.426(19)	70.865(2)	110.3030(10)	119.315(3)
γ (°)	90	86.3520(10)	67.820(10)	105.059(16)	85.8460(10)	90.0	90
V ($Å^3$)	911.0	705.54	1328.95	655.9	743.89	1375.26	1415.03
Z	4	2	4	2	2	4	4
$D_{calcd.}$ (g/cm^3)	1.307	1.202	1.266	1.283	1.258	1.359	1.32
Range of 2θ	4–50	3–27	3–27	3–27	4–27	3–27	3–27
Collected Reflections	1590	3117	9739	2970	3228	9080	3177
Independent Reflections	1590	3117	5866	2969	3228	3086	3177
R/R_w (F)	0.0409/0.1196	0.0568/.1590	0.0446/0.1000	0.0548/0.1345	0.0675/0.1684	0.0576/0.1558	0.060/0.106
R/R_w (F^2) (all data)	0.0595/0.1334	0.0837/0.1708	0.0845/0.1176	0.1195/0.1604	0.0805/0.1776	0.0813/0.1725	0.144/0.127
GOOF	1.016	1.019	0.984	1.030	1.173	1.051	1.063
parameters	119	218	464	233	259	191	251
(ρmin (e Å − 3)	−0.194	−0.291	−0.136	−0.222	−0.420	−0.270	−0.120
(ρmax (e Å − 3)	0.273	0.355	0.170	0.195	0.453	0.375	0.125

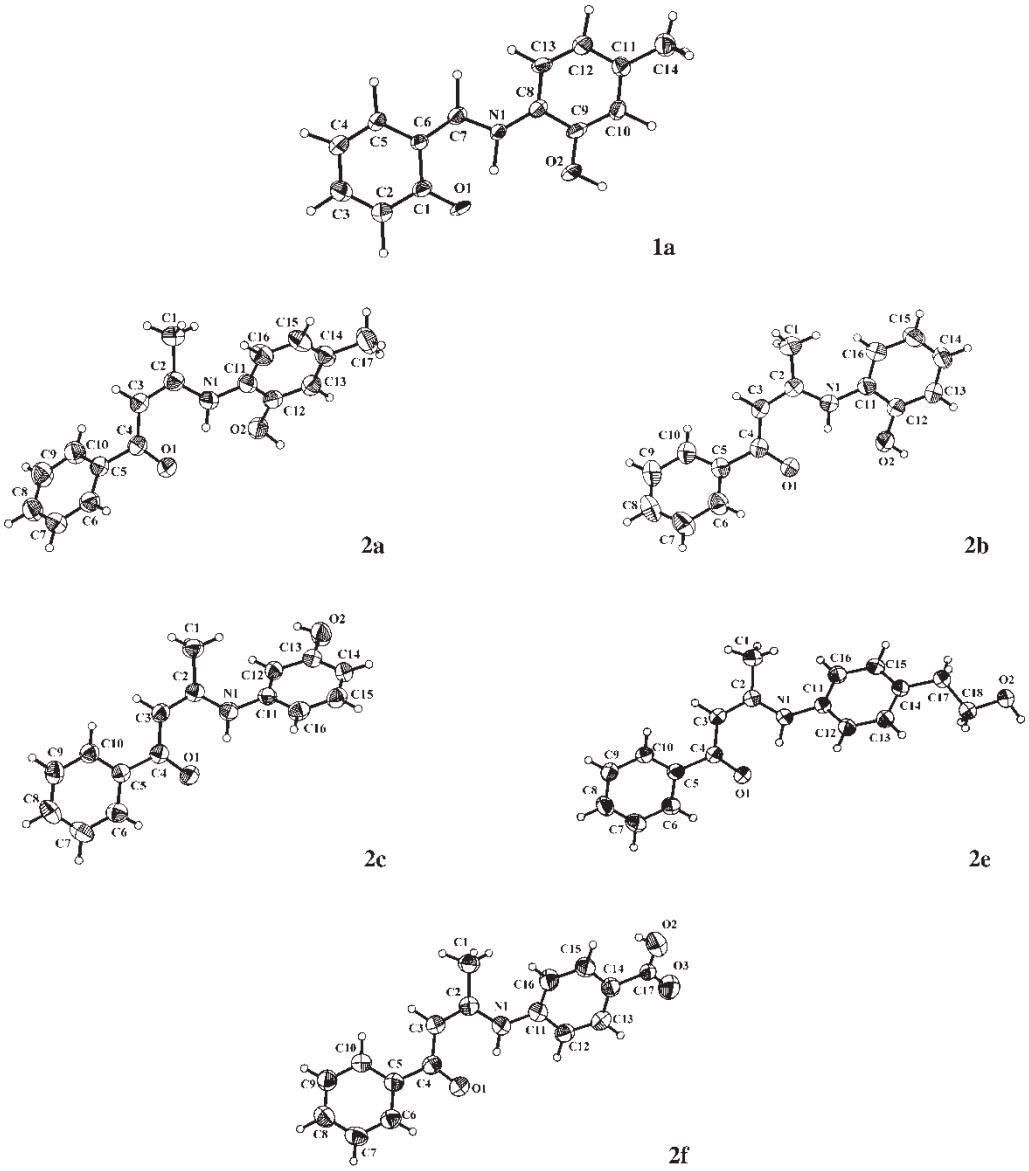

FIGURE 10 Perspective molecular view for **1a**, **2a**, **2b**, **2c**, **2e** and **2f**. The ellipsoids are shown at the 50% probability level.

for **A-keto**, **B** and **C** 1.310(1) Å, 1.3490(17) Å and 1.354(4) Å, respectively.

The torsion angle value of **1a** (11.18(8)°) for the C(7)—N(1)—C(8)—C(13) fragment shows that the aromatic moieties are not as coplanar as in the **A-enol** 3.57(3)°, but they are less twisted than **B** and **C**, 39.77(17)° and 41.58(5)°, respectively. The X-ray structure of **1a** showed the formation of a strong intramolecular N(1)H···O(1) hydrogen bond between the NH and the oxygen atom of the keto group [N(1)···O(1) = 2.586(5) Å, N(1)—H···O(1) = 150(4)°] to form an intramolecular six membered ring S(6) [27]. Both the short N(1)···O(1) distance and the N(1)—H···O(1) angle are indicative of the strength [25] of the hydrogen bond formed (Fig. 11). The same type of contacts are also observed in photochromic derivates **B**, **C** and N-*o*-hydroxybenzylideneaniline, however, in the case of the thermochromic derivative the intermolecular interaction involves the imine proton. The geometric parameters of hydrogen bonding interactions are listed in Table IV. The ketoenamine tautomer in **1a** is also stabilized by the formation of an O(2)—H···O(1) hydrogen bonding interaction between the phenolic OH and the oxygen atom of the keto group in a neighboring molecule (Fig. 11) [28]. This intermolecular hydrogen bond also leads to a variation in the bond distance for the O(2)—C(9)—C(8)—N(1) fragment, 1.361(6) Å (O—C), 1.404(7) Å (C—C) and 1.398(6) Å (C—N) distances, compared with the values obtained by Elerman [29] in N-*o*-hydroxybenzylideneaniline [1.411(5) Å, 1.376(6) Å and 1.418(8) Å], wherein intermolecular hydrogen bond was not observed.

TABLE III. Selected bond distances and deslocalization parameters for the N—C—C—C—O fragment in compounds **1a**, **A-Keto**, **B**, **C**, **2a–c** and **2e–f′**.

	N—C(7)	C(7)—C(6)	C(6)—C(1)	C(1)—O(1)	C(6)—C(5)	C(1)—C(2)	λ	Del(%)
1a	1.323(6)	1.395(7)	1.426(7)	1.297(6)	1.419(7)	1.405(8)	0.50	100
A-Keto[a]	1.308(1)	1.425(2)	1.433(2)	1.310(1)	1.419(3)	1.376(3)		
B	1.2888(18)	1.440(2)	1.4197(19)	1.3490(17)	1.404(2)	1.386(2)		
C	1.282(4)	1.448(5)	1.418(5)	1.354(4)	1.385(5)	1.411(5)		
	N(1)—C(2)	**C(2)—C(3)**	**C(3)—C(4)**	**C(4)—O(1)**	**C(4)—C(5)**	**N(1)—C(11)**		
2a	1.341(3) *1.41*	1.385(3) *1.55*	1.415(3) *1.38*	1.265(2) *1.55*	1.497(3)	1.427(2)	0.42	84
	1.337(2) *1.43*	1.381(2) *1.58*	1.412(2) *1.40*	1.2650(17) *1.55*	1.495(2)	1.421(2)	0.42	84
2b	1.3401(19) *1.41*	1.382(2) *1.57*	1.408(2) *1.42*	1.2671(17) *1.54*	1.493(2)	1.426(2)	0.43	86
2c	1.325(3) *1.50*	1.389(3) *1.53*	1.413(3) *1.40*	1.259(3) *1.59*	1.493(4)	1.424(3)	0.44	88
2e	1.338(2) *1.42*	1.384(2) *1.55*	1.417(2) *1.37*	1.260(2) *1.58*	1.495(2)	1.422(2)	0.41	82
2f	1.355(3) *1.33*	1.376(3) *1.61*	1.433(3) *1.29*	1.251(2) *1.63*	1.500(3)	1.401(2)	0.34	68
2f′	1.355(2) *1.33*	1.373(3) *1.63*	1.421(3) *1.35*	1.255(2) *1.61*	1.498(2)	1.403(2)	0.36	72

[a] Values reported for 90% of the keto form.

The above mentioned hydrogen bonding interactions, lead to the formation of infinite zigzagging $C_2^1(7)$ chains (Fig. 12) that propagate along the *b* axis. Dimers formed by $C(sp^3)$—H···π interactions between one of the methyl protons and the centroid of the cyclohexadienone type ring [C(14)···Cg = 3.523(7) Å, C(14)—H(14A)···Cg = 132(4)°, symmetry code: 1 − x, y, 1 − z], contribute to the supramolecular structure.

X-ray Study of Compounds 2a–c and 2e–f′

The X-ray diffraction analysis corroborates the molecular structures of derivatives **2a–c** and **2e–f′** which are shown in Fig. 10, and selected bond lengths are listed in Table III. Comparison with the standard $N(sp^3)$—$C(sp^2)$=$C(sp^2)$—$C(sp^2)$=$O(sp^2)$ values which are 1.44 Å, 1.33 Å, 1.48 Å and 1.20 Å, respectively [26], reveals that the N—C—C—C—O fragment in these molecules has partial single and double bond character. Besides, the N—C—C—C—O fragment is connected by a N—H···O hydrogen bond forming a delocalized six membered ring S(6), where C(4) shows deviations of 0.057 Å (**2a**), −0.016 Å (−0.022) (**2b**), 0.010 Å (**2c**), 0.019 Å (**2e**), 0.017 Å (**2f**) and 0.018 Å (**2f′**) from the mean N—C—C—C—O plane. Hydrogen bonding geometrical parameters are listed in Table IV. The N···O bond length values for the N—H···O interaction vary from 2.618(2) Å to 2.683(3) Å, corresponding to a strong intramolecular hydrogen bond [$\Sigma r_{VDW}(N,O) = 3.1$ Å] with N—H···O angles in the range of 135(2)° to 144(3)°. Finally, it is worthy to mention that both phenyl rings are out of the N—C—C—C—O mean plane with C(2)—N(1)—C(11)—C(12) torsion angle values of −122.2(2)° (**2a**), −141.1(2)° (−121.5(2)°) (**2b**), 131.1(3)° (**2c**), 139.45(19)° (**2e**), 147.93(19)° (**2f**) and −153.80(19)° (**2f′**) and C(3)—C(4)—C(5)—C(6) torsion angle values of −144.9(2)° (**2a**), −163.16(18)°

FIGURE 11 Molecular interactions in **1a**, the atoms involved in H-bonding are shown in black.

TABLE IV Geometric parameters for Hydrogen bonding and other interactions in compounds **1a**, **2a–c** and **2e–f′**.

Comp.	D—H···A	D—H	H···A	D···A	D—H···A
1a	N(1)—H(1)···O(1)	1.02(5)	1.66(5)	2.592(5)	150(4)
	O(2)—H(21)···O(1)[a]	0.94(6)	1.65(6)	2.582(5)	173(6)
	C(14) —H(14A)···Cg(1)[a]	0.94(7)	2.89(6)	3.523(7)	132(4)
2a	N(1)—H(2)···O(1)	0.96(3)	1.88(3)	2.650(2)	135(2)
	O(2)—H(12)···O(1)[b]	1.02(4)	1.67(4)	2.654(2)	163(3)
	C(1)—H(1)···Cg(1)[c]	0.96	2.68	3.625(3)	160
	C(6)—H(6)···Cg(2)[d]	0.93	2.82	3.804(6)	140
2b	N(1)—H(2)···O(1)	0.91(2)	1.92(2)	2.673(2)	139(3)
	O(2)—(12)···O(1)[e]	0.85(3)	1.83(3)	2.637(2)	158(3)
	N(2)—H(18)···O(3)	0.87(3)	2.00(3)	2.683(3)	135(3)
	O(4)—H(29)···O(3)[f]	0.93(4)	1.76(3)	2.641(2)	158(3)
	C(9)—H(9)···O(2)[g]	0.93	2.56	3.341(4)	142
	C(26)—H(26)···O(4)[c]	0.93	2.56	3.286(4)	135
	C(7)—H(7)···Cg(2)[h]	0.93	2.90	3.3715(3)	148
2c	N(1)—H(2) ···O1	0.85(6)	1.91(6)	2.626(4)	141(4)
	O(2)—H(2A)···O1[i]	0.82	2.21	2.704(4)	119
	C(1)—H(1C).Cg(1)[i]	0.96	2.78	3.668(4)	151
	C(15)—H(15)···Cg(1)[d]	0.95	2.88	3.672(4)	135
2e	N(1)—H(2)···O(1)	0.95(3)	1.79(3)	2.618(2)	144(3)
	O(2)—H(20)···O(1)[j]	0.94(4)	1.88(4)	2.790(2)	163(3)
	C(7)—H(7)···Cg(2)[k]	1.02(3)	2.84(3)	3.650(2)	138(2)
	C(10)—H(10)···Cg(2)[i]	0.974(18)	2.85(2)	3.626(2)	137.0(17)
	C(16)—H(16)···Cg(1)[l]	0.96(3)	2.70(3)	3.503(2)	141.5(19)
2f	N(1)—H(1B)···O(1)	0.96	1.82	2.638(2)	141
	C(6)—H(2)···O(3)[f]	0.93	2.50	3.416(3)	169
	C(13) —H(13)···O(1)[m]	0.93	2.48	3.221(3)	137
	C(12) —H(12)···Cg(1)[m]	0.93	3.434	3.27(1)	175
2f′	N(1)—H(2)···O(1)	0.97(2)	1.79(2)	2.618(2)	142(2)
	O(3)—H(17)···O(2)[n]	1.05(4)	1.60(4)	2.6431(3)	173(3)
	C(1)—H(1B)···O(2)[o]	0.99(2)	2.57(3)	3.531(4)	162.9(18)

Symmetry codes: (a) [1 − x, 1/2 + y, 3/2 − z], (b) [− x, 2 − y, − z], (c) [1 − x, 1 − y, − z], (d) [x, y, − 1 + z], (e) [1 − x, − y,1 − z], (f) [− x, 1 − y, − z], (g) [2 − x, − y, 1 − z], (h) [1 + x, − 1 + y, z], (i) [1 + x, y, z], (j) [x, 2 − y, − z], (k) [1 + x, y, − 1 + z], (l) [1 − x, 2 − y, − z], (m) [− 1 + x, 3/2 − y, − 1/2 + z], (n) [− 1 − x, − y, − 1 − z], (o) [1/2 + x, 1/2 − y, 1/2 + z].

(−166.57(16)°) (**2b**), 158.3(3)° (**2c**), 155.60(17)° (**2e**), 158.21(17)° (**2f**) and 158.21(17)° (**2f′**) and these twist conformations could be responsible for the photochromic properties [30,31]. These last results contrast with the planarity of molecule **1a**. The above mentioned findings as a whole suggest the presence of a resonance assisted by hydrogen bonding phenomena in this set of compounds, as will be discussed below.

The supramolecular structure is directed by the nature of the substituent group in the aniline fragment. Compounds **2a–c** and **2e**, all of them bearing a hydroxy group, present the intermolecular O(2)—H···O(1) hydrogen bonding interaction between the OH group, as donor, and the oxygen atom from the carbonyl group, as the acceptor, as a common pattern. Both intramolecular N(1)—H···O(1) and intermolecular O(2)—H···O(1) interactions leads to the main hydrogen bonding motifs, which mainly depend on the OH position in the aniline ring. In all cases the supramolecular structure is complemented by intermolecular C—H···A (A═O, π) interactions [32]. The geometric parameters for these interactions are listed in Table III.

Thus, compounds **2a** and **2b**, both of them derived from *o*-hydroxyaniline, form centrosymmetric $R_2^2(14)$ rings interlinked through C(1)—H(1)···Cg(1) and C(6)—H(6)···Cg(2) for **2a** (Fig. 13) and C(9)—H(9)···O(2), C(26)—H(26)···O(4) and C(7)—H(7)···Cg(2) for **2b** (Fig. 13) [Cg(1) and Cg(2) are the centroids of the

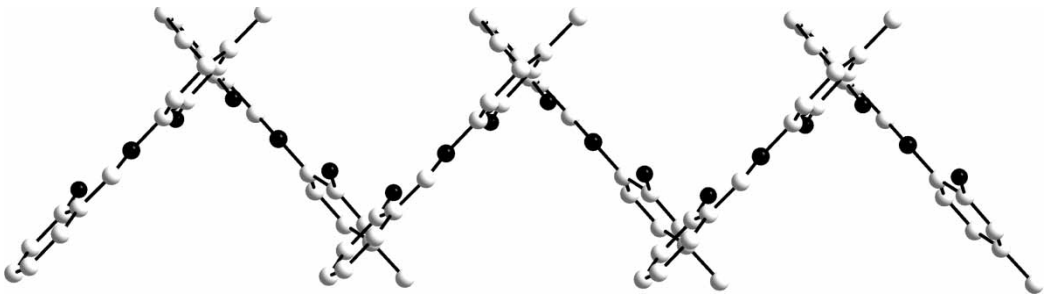

FIGURE 12 Supramolecular structure of compound **1a**. Formation of chains through hydrogen bonding interaction.

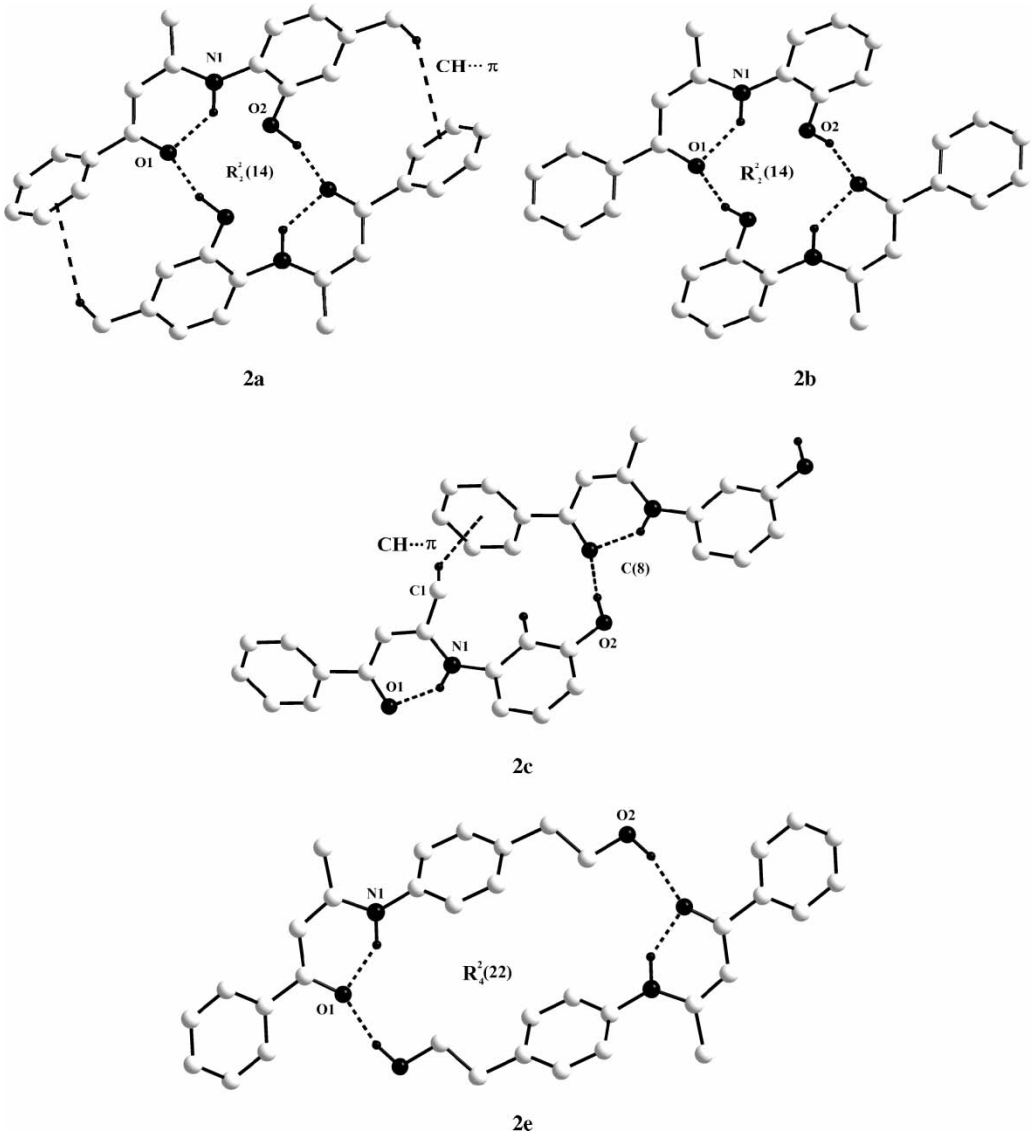

FIGURE 13 Molecular interactions in **2a**, **2b**, **2c** and **2e**, the atoms involved in H-bonding are shown in black.

phenyl ketone and aniline rings, respectively]. The X-ray structure of a polymorph of **2b** reported by Hall [33] in 1991, and crystallized from ethyl alcohol,

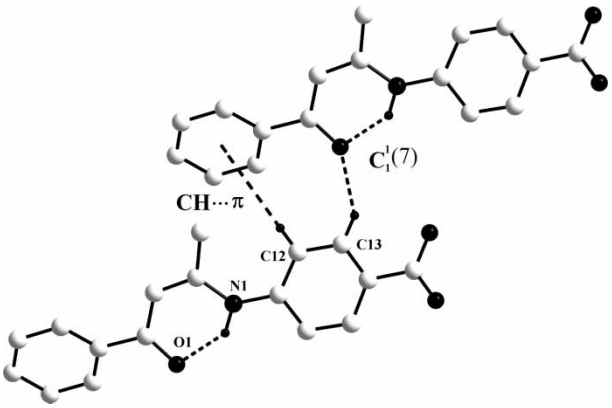

FIGURE 14 Molecular interactions in **2f**, the atoms involved in H-bonding are shown in black.

shows an intramolecular NH···O and an intermolecular EtOH···O hydrogen bond. In the case of compound **2e** (*p*-ethanolaniline derivative), a larger $R_4^2(22)$ centrosymmetric ring (Fig. 13) is the observed motif, whereas in compound **2c** (*m*-hydroxyaniline derivative) C(8) infinite chains, developing along the *a* axis (Fig. 13), are formed. The supramolecular structure is complemented by C(1)—H(1C)···Cg(1) and C(15)—H(15)···Cg(1) for **2c** and C(7)—H(7)··· Cg(2), C(10)—H(10)···Cg(2) and C(16)—H(16)··· Cg(1) for **2e**.

The substitution of a carboxylic acid at the *para* position to the amine allowed the formation of two polymorphs, in both of them the N—H···O resonance assisted hydrogen bond is formed, as discussed before, however, the supramolecular structure of each polymorph is achieved through the participation of very different sort of interactions. In the case of polymorph **2f**, weak C(sp^2)—H···A (A═O, π)

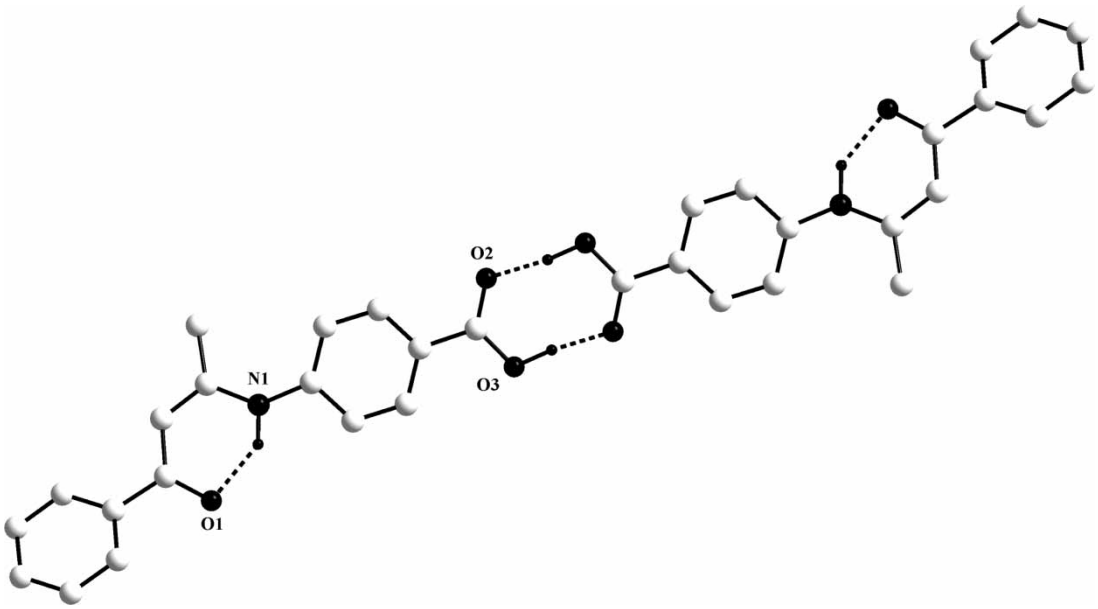

FIGURE 15 Molecular interactions in **2f′**, the atoms involved in H-bonding are shown in black.

interactions prevail, whereas in polymorph **2f′**, hard whereas in polymorph **2f**, O—H···O hydrogen bonding does it.

$R_2^2(26)$ dimers are formed through the participation of C(6)—H(2)···O(3) interactions which are interlinked by C(13)—H(13)···O(1) interactions that develop along the *b* axis (Fig. 14).

In the second polymorph **2f′**, centrosymmetric dimers are formed through the —COOH group participation, which plays the role of both hydrogen bonding donor and acceptor to form $R_2^2(8)$ rings [O(3)—H···O(2)] (Fig. 15). This kind of system is frequently found in systems that have carboxylic acid groups and present the phenomena of resonance assisted by hydrogen bonding. There is also the short contact C(1)—H(1B)···O(2) which connects the dimers in the family of planes (Fig. 15).

Analysis of RAHB for Derivatives 1a, 2a, 2b 2c, 2e and 2f

Table III summarizes the bond distance values for the N(sp^2)—C(sp^2)-C(sp^2)—C(sp^2)—O(sp^2) fragment (Fig. 16), the bond number is shown in italics

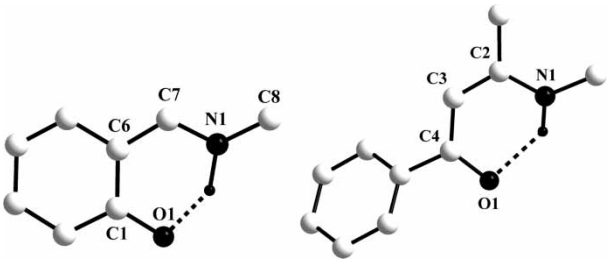

FIGURE 16 Fragments involved in proton transfer for arylimines and arylenaminones.

and was calculated using Pauling's equation, $D(n) = D(1) - 0.60 \log n$ [34]. These values were employed to calculate the π-delocalization parameter λ ($\lambda = (1/4)\ [n(1) - 1] + [2 - n(2)] + [n(3) - 1] + [2 - n(4)]$ [35]. Del% values were calculated using the equation $\text{Del\%} = 100(1 - |2\ \lambda\ - 1|)$ [36] and interpreted in terms of structures, thus the extreme geometries are characterized by the same Del% = 0, however λ = 0 is found for ketoenamine and λ = 1 for enolimine tautomers; a fully π-delocalized structure has Del% = 100 for λ = 0.5.

The arylimine **1a** showed a λ = 0.5 indicating complete delocalization, this is corroborated by a large Del% value. In this type of derivatives the N(sp^2)—C(sp^2)—C(sp^2)—C(sp^2)—O(sp^2) fragment is part of an aromatic unit, favoring the structural and electronic requirements, although the most important factor is the second OH unit which helps to stabilize the keto-enamine tautomer. The calculated bond number values for the π-system fragment in **2a**–**2c** and **2e**, showed average values between *1* and *2* indicating a certain electronic delocalization, this is corroborated by the λ values of 0.5 except for derivative **2f** (0.34 and 0.36) which presents the shortest Del% values.

Table IV summarizes the data related to hydrogen bonding in compounds **2a**–**2c**, **2e** and **2f**. The values for the N—O distances are in the range from 2.618(2) Å and 2.683(3) Å, typical of this type of derivatives (2.53–2.72 Å). Compound **2e** presents the shortest N—O (2.618(2) Å) and NH···O (1.79(3) Å) distances and **2b** the largest ones 2.683(3) Å for N—O and 2.00(3) Å for NH···O. On the other hand, for **1a** the N—O distance (2.592 Å) presents a slightly larger value compared with the average value (2.46–2.57 Å) [25].

CONCLUSION

The experiments in the solid state and in solution for enamines **2a**–**2f** allow to conclude that in solution the keto-enamine tautomer is the most stable species. In turn the enol-imine species is the most stable form for imine **1a** in solution while X-ray diffraction analysis showed that in solid state the keto-enamine is the preferred species. For **2b**, the tautomeric Keto-enamine (O═C—C═C—N—H···): Enol-imine (···HO—C═C—C═N) equilibrium was confirmed by VT-NMR based on the chemical shift of NH and H-1 (δ) behavior in different solvents. Correlation of the proton NMR signal whit temperature showed that in non polar solvents and at low temperatures, the proton NMR signals for H-3 and H-1 shift to high frequency. The X-ray diffraction analysis allowed to established the structure of derivatives **2a**–**2c**, **2e** and **2f** which correspond to the keto-enamine species; moreover, the NH absorption band in IR, as well as the N—O and NH···O distance values confirm the existence of strong hydrogen bonds. The distance values obtained from the X-ray analysis for the N(1)—C(2)—C(3)—C(4)—O(1) fragment allowed to calculate the percent delocalization (Del%) evidencing greater delocalization in **2a**–**2e** while **2f** presents the smallest value. Comparison of the Del% with N—O and NH···O distances shows no correlation, therefore, in this case, neither H-bonding nor substituents at the *para* position of the aniline fragment promote delocalization. The X-ray analysis for **1a** showed an intramolecular NH···O (1.66(5) Å) and strong intermolecular OH···O, characteristic of RAHB ring formation with the phenyl group. The Del% valued indicated complete delocalization however the N—O distance 2.592(5) Å is slightly longer than the value (2.57 Å) reported for this type of derivates [25]. Finally, the existence of a second intermolecular proton transfer plays an important role to stabilize the keto-enamine tautomer or to promote the conversion to this tautomer when the arylimine is irradiated under UV.

Supplementary Material

For compounds **1a**, **2a**, **2b** **2c**, **2e** and **2f** full crystallographic data were submitted as CIF files with the Cambridge Crystallographic Data Center, CCDC Nos. 638598 for **1a**, 638592 for **2a**, 638593 for **2b**, 638594 for **2c**, 638597 for **2e** and for **2f** 638595 and 638596.

Acknowledgements

The authors thank CONACyT for financial support and the scholarship to M. Rodriguez. Thanks are given to Consejo Superior de la Investigación Científica in Spain for the Cambridge Crystallographic Data Base license, to M. L. Rodriguez for NMR spectra, R. Yepez for IR, M. A. Leyva for X-ray analysis and G. Cuellar for MS.

References

[1] Dossier, R. H.; Bogolmolni, R. A.; Stoeckenius, W. *Biophys. J.* **1995**, *15*, 955.
[2] Garnovskii, A. D.; Nivorozhkin, A. L.; Minkin, V. *Coord. Chem. Rev.* **1993**, *126*, 1.
[3] Cohen, M. D.; Schmidt, G. M.; Flavian, S. *J. Chem. Soc.* **1964**, 2041.
[4] Hadjousdis, E.; Vittorakis, M.; Moustakali-Mavridis, I. *Tetrahedron* **1987**, *43*, 1345.
[5] Ogawa, K.; Kasahara, Y.; Ohtani, Y.; Harada, J. *J. Am. Chem. Soc.* **1998**, *120*, 7107.
[6] Ogawa, K.; Harada, J.; Fujirawa, T.; Yoshida, S. *J. Phys. Chem. A* **2001**, *105*, 3425.
[7] Sliwa, M.; Létard, S.; Malfant, I.; Nierlich, M.; Lacroix, P.; Asahi, T.; Masuhara, H.; Yu, P.; Nakatani, K. *Chem. Mater.* **2005**, *17*, 4727.
[8] Edafiogho, I. O.; Phillips, O. A.; Abdel-Hamid, M.; Ali, A. A. M.; Matowe, W. C.; El-Hasim, A.; Kobian, S. B. *Bioorg. Med. Chem.* **2002**, *10*, 593.
[9] Kuicki, M.; Bassyouni, H. A. R.; Codding, P. W. *J. Mol. Struct.* **2000**, *525*, 141.
[10] Bilbao, E. R.; Alvarado, M.; Masaguer, C. F.; Raviña, E. *Tetrahedron Lett.* **2002**, *43*, 3551.
[11] Abdel-Zaher, A.; El-Khair, A. A. *Tetrahedron* **2003**, *59*, 8463.
[12] Peng, X.; Wu, Y.; Fan, J.; Tian, M.; Han, K. *J. Org. Chem.* **2005**, *70*, 10524.
[13] Lin, Z.; Ou, S.; Duan, C.; Zhang, B.; Bai, Z. *JCS Chem. Comm.* **2006**, 624.
[14] Fonseca, T. L.; de Oliveira, H. C. B.; Amaral, O. A. V.; Castro, M. A. *Chem. Phys. Lett.* **2005**, *413*, 356.
[15] Gilli, G.; Bellci, F.; Ferretti, V.; Bertolasi, V. *J. Am. Chem. Soc.* **1989**, *111*, 1023.
[16] Gilli, G.; Gilli, P. *J. Mol. Struct.* **2000**, *552*, 1.
[17] Cindrić, M.; Novak, T. K.; Užarević, K. *J. Mol. Struct.* **2005**, *750*, 135.
[18] Rybarczyk-Pirek, A. J.; Grabowski, S. J.; Nawrot-Modranka, J. *J. Phys. Chem. A* **2003**, *107*, 9232.
[19] Steiner, T. *JCS Chem. Commun.* **1998**, 411.
[20] González, L.; Mó, O.; Yañez, M. *J. Org. Chem.* **1999**, *64*, 2314.
[21] See *Chem. Rev.* **2005**, *105*, 3513–3561.
[22] Wachter, N.; Detmer, C. *Org. Lett.* **1999**, *1*, 795.
[23] Sheldrick, G. M. *SHELXL-97, Program for Crystal Structure Solution*; University of Göttigen: Germany, 1997; p Germany.
[24] (a) Barba, V.; Cuahutle, D.; Santillan, R. Farfán, N. *Can. J. Chem.* **2001**, *79*, 1229, b) Xue, S.; Yu, S.; Deng, Y.; Wulff, W.D. *Angew, Chem. Int. Ed.* **2001**, *40*, 2271..
[25] Gilli, P.; Bertolasi, V.; Ferretti, V.; Gilli, G. *J. Am. Chem. Soc.* **2000**, *122*, 10405.
[26] Allen, F. H.; Kennard, O.; Watson, D. G.; Brammer, L.; Orpen, A. G.; Taylor, R. *Typical distances: organic compound in international Tables for crystallography* **1992**.
[27] Bernstein, J.; Davis, R. E.; Shimoni, L.; Chang, N.-L. *Angew. Chem. Int. Ed. Engl.* **1995**, *34*, 1555.
[28] Cohen, M. M.; Flavian, S. *J. Chem. Soc. B* **1967**, 321.
[29] Elerman, Y. *Acta Cryt. Sec. C* **1995**, *51*, 2344.
[30] Moustakali-Mavridis, I.; Hadjoudis, E.; Mavridis, A. *Acta Cryst. B* **1978**, *34*, 3709.
[31] Bregman, J.; Leiserowitz, L.; Osaki, K. *J. Chem. Soc. Jph.* **1964**, 2086.
[32] Umezawa, Y.; Tsuboyama, S.; Honda, K.; Uzawa, J.; Nishio, M. *Bull. Chem. Soc. Jpn.* **1998**, *71*, 1207.
[33] Hall, S. R.; Allen, F. H.; Brown, I. D. *Acta Cryst. A* **1991**, *47*, 655.
[34] Pauling, L. *The Nature of the Chemical Bond*; 3rd ed., Cornell University Press: Ithaca, NY, 1960.
[35] Gilli, P.; Bertolasi, V.; Pretto, L.; Ferreti, V.; Gilli, G. *J. Am. Chem. Soc.* **2004**, *126*, 3845.
[36] Bertolasi, V.; Pretto, L.; Gilli, G.; Gilli, P. *Acta Cryst.* **2006**, *B62*, 850.